Effect of tolerance factor and A-site cations disorder on transport properties of $A'_{1-x}A''_xCoO_{3-\delta}$ perovskites (A' = Ho, Er; A'' = Ca, Sr)

A.A.Kozlovskii, V.F.Khirnyi, A.V.Semenov, V.M.Puzikov, T.G.Deineka, O.V.Gaiduk[*], Yu.N.Chiang[**]

Institute for Single Crystals, STC "Institute for Single Crystals", National Academy of Sciences of Ukraine, 60 Lenin Ave., 61001 Kharkiv, Ukraine
[*] State Scientific Institution, STC "Institute for Single Crystals", 60 Lenin Ave., 61001 Kharkiv, Ukraine
[**] B.Verkin Institute for Low Temperature Physics and Engineering, National Academy of Sciences of Ukraine, 47 Lenin Ave., 61103 Kharkiv, Ukraine

Temperature dependences of conductivity for $Ho_{1-x}Sr_xCoO_{3-\delta}$, $Er_{1-x}Sr_xCoO_{3-\delta}$, $Ho_{1-x}Ca_xCoO_{3-\delta}$ and $Er_{1-x}Ca_xCoO_{3-\delta}$ ($x = 0.15, 0.25, 0.35, 0.45, 0.55, 0.65, 0.75, 0.85, 0.95$) having the ABO_3 perovskite structure have been studied in the $T>77$ K temperature region. All the compounds studied are characterized by hopping conduction with the temperature dependence of conductivity $\rho(T) = \rho_\infty exp(T_0/T)^{1/n}$. Depending on the distribution dispersion σ^2 of A cationic radii, different types of the hopping conduction are realized. In most samples, the conduction occurs as the variable range hopping conduction in the Mott mode ($n = 4$). In the $Ho_{1-x}Sr_xCoO_{3-\delta}$ system, a transition to the hopping conduction over the nearest sites occurs as the σ^2 increases ($n = 1$); while in the $Er_{1-x}Sr_xCoO_{3-\delta}$, to the Efros-Shklovsky mode ($n = 2$). In $Ho_{1-x}Sr_xCoO_{3-\delta}$ samples, the spin conduction channel arises as the temperature rises up to 190–270 K due to cobalt ion transition into excited state.

В области температур $T>77$ К исследованы температурные зависимости удельного электрического сопротивления ρ керамик $Ho_{1-x}Sr_xCoO_{3-\delta}$, $Er_{1-x}Sr_xCoO_{3-\delta}$, $Ho_{1-x}Ca_xCoO_{3-\delta}$ и $Er_{1-x}Ca_xCoO_{3-\delta}$ ($x = 0,15; 0,25; 0,35; 0,45; 0,55; 0,65; 0,75; 0,85; 0,95$), обладающих структурой перовскита ABO_3. Изученные соединения характеризуются прыжковой проводимостью с температурной зависимостью электросопротивления $\rho(T) = \rho_\infty exp(T_0/T)^{1/n}$. В зависимости от дисперсии распределения σ^2 радиусов А-катионов реализуются различные типы прыжковой проводимости. В большинстве образцов проводимость осуществляется по механизму прыжковой проводимости с переменной длиной прыжка в режиме Мотта ($n = 4$). В системе $Ho_{1-x}Sr_xCoO_{3-\delta}$ при увеличении величины σ^2 происходит переход к прыжковой проводимости между ближайшими соседями ($n = 1$), а в системе $Er_{1-x}Sr_xCoO_{3-\delta}$ — к режиму Эфроса-Шкловского ($n = 2$). В образцах $Ho_{1-x}Sr_xCoO_{3-\delta}$ при повышении температуры до 190–270 К обнаружено появление спинового канала проводимости, связанное с переходом ионов кобальта в возбужденное состояние.

During several last years, ever more works are published aimed at cobalt based metal oxide compounds (cobaltites). This is due to the properties of cobaltites typical of other strongly correlated systems (the dielectric-metal transitions, charge and or-

bital superstructures, strong dependence of conductivity on external magnetic field, superconductivity in sodium cobaltite hydrate, etc.) as well as some specific features thereof, in particular, a high thermo-e.m.f. [1].

In cobaltites having the ABO_3 perovskite structure, cobalt ion in the center of CoO_6 octahedron is surrounded by negatively charged oxygen ligands. Due to the crystal field effect, the fivefold degenerate $3d$-orbitals of Co^{3+} ion are split into threefold degenerate t_{2g} levels and doubly degenerate e_g ones with corresponding energy values ε_{t2g} and ε_{eg}, $\varepsilon_{eg} > \varepsilon_{t2g}$. That is why electrons occupy at first the t_{2g} orbitals and then the e_g ones. Depending on the relation between the splitting energy in the crystal field $\Delta = \varepsilon_{eg} - \varepsilon_{t2g}$ and the intraatomic exchange interaction energy, the cobalt ion may be in different spin states, namely, low-spin (LS), high-spin (HS) and intermediate spin (IS) ones [2] that affect the transport and magnetoresistive properties of cobaltites [3].

At present, it is the $La_{1-x}Sr_xCoO_{3-\delta}$ system that is the best explored among cobaltites. The initial compound $LaCoO_3$ is a non-magnetic dielectric where the cobalt ion passes out of the LS state into the IS one as the temperature rises up to 100 K. The introduction of Sr^{2+} ions having a considerable larger radius than La^{3+} results in stabilization of the excited cobalt ion states [2]. In this case, the kinetic properties are changed dramatically: depending on the Sr content, the samples may be semiconductors or conductors, the electron phase sseparation and giant negative magnetoresistance arise [4]. The kinetic phenomena in other rare-earth cobaltites were studied much less comprehensively. Moreover, the concentration effect of different rare-earth elements on kinetic features in A-substituted rare-earth cobaltites is studied insufficiently.

The kinetic properties of perovskite-like A-substituted rare-earth cobaltites are defined by three groups of factors [5]. Those are, first, the charge carrier concentration that depends on the doping level and the substituting cation valence. Second, it is the average raduis $<r_A>$ of the A site cations. That parameter defines the chemical pressure in the system and thus the crystal field affecting the Co cation. To estimate the influence extent of $<r_A>$ value, a geometric parameter can be used describing the perovskite lattice straining, i.e., the Goldschmidt tolerance factor [6]:

$$t = (<r_A> + r_O)/(\sqrt{2})(<r_B> + r_O), \qquad (1)$$

where $<r_B>$ is the average radius of B-cations (in our case, cobalt ones); r_O, oxygen ion radius.

The third factor affecting the kinetic properties of perovskite-like A-substituted compounds is the distribution disorder of different kind ions occupying the site A that is defined by thereof size mismatch. Quantitatively, that parameter can be presented as the variance of the distribution of A-cation ionic radii [7]:

$$\sigma^2 = \sum y_i r_i^2 - \left(\sum y_i r_i\right)^2, \qquad (2)$$

where y_i is the concentration of i-th kind A-cations ($\sum y_i = 1$). When there is one cation kind only, $\sigma^2 = 0$. The ioniccc size mismatch factor ia as a rule neglected when considering the kinetic properties of perovskites. The effect of σ^2 on the charge and magnetic order in manganites was reported in [8−10].

The aim of this work was to study the transport properties of $A'_{1-x}A''_xCoO_{3-\delta}$ rare-earth cobaltites ($A' = Ho, Er; A'' = Ca, Sr$) within a wide concentration range of rare-earth dopants ($0.15 \leq x \leq 0.95$). The compositions so selected make it possible to determine the correlation degree of the charge carrier transport with each of the three above-mentioned factors, since the strontium and calcium are of the same valence, the ionic radii of rare-earth elements are close to one another ($r_{Ho} = 0.901$ Å, $r_{Er} = 0.89$ Å) while those of alkali-earth ones differ considerably ($r_{Sr} = 1.18$ Å, $r_{Ca} = 1.0$ Å) [11]. Moreover, it is of interest to study the intensification of the charge carrier localization effects due to introduction of holmium and erbium having ionic radii shorter than lanthanum ($r_{La} = 1.032$ Å).

The ceramic samples of $Er_{1-x}Sr_xCoO_{3-\delta}$, $Ho_{1-x}Sr_xCoO_{3-\delta}$, $Er_{1-x}Ca_xCoO_{3-\delta}$ and $Ho_{1-x}Ca_xCoO_{3-\delta}$ ($x = 0.15, 0.25, 0.35, 0.45, 0.55, 0.65, 0.75, 0.85, 0.95$) were synthesized by the standard solid phase technique. The samples obtained were shaped as rectangular parallelepipeds of $0.25 \times 0.55 \times 2.5$ cm^3. According to X-ray analysis (DRON-50, Cu K_α emission), the ceramics were single-phase ones and had the perovskite-like crystal structure [12].

The chemical composition and oxygen index of the samples were determined by chemical analysis. The total Co contents was determined using a redox reaction be-

tween phenanthroline complexes of cobalt (II) and iron (II). The rare-earth element conteats were determined by direct complexoment in weak acidic medium with xylenol orange indicator and those of alkaliearth ones, by inverse titration in alkali medium with methyl thymol thymol blue. The cation indices determined coincided with stoichiometric ones. The oxygen deficiency index $\delta = 0.4\pm0.06$.

The conductivity ρ was measured by the standard four-probe dc technique in the 77–300 K temperature range (for some samples, up to 770 K). The measuring current passed along the sample. Indium contacts were applied across the sample using the ultrasound soldering. The distance between the potential outputs was 10 mm. The measuring current was 10 mA. The measurements were done under the sample heating.

The magnetic state of the samples was controlled by measuring the ac magnetic susceptibility χ_{AC} using a setup similar to the Hartshorn bridge. The amplitude of alternating (modulating) magnetic field was $H(t) = H_{AC}\cos(\omega t)$ at $H_{AC} = 3$ Oe and frequency $\omega/2\pi = 5$ kHz.

The $<r_A>$, t and σ^2 values were calculated using the data from [11]. The effective radius of A-site cations and the tolerance factor increase as the alkali-earth element concentration rises, their values always are considerably lower for Ca containing samples than for Sr containing ones. At the same time, the tolerance factors and effective radii of A-site cations differ only slightly for the Ho and Er ceramics doped with the same alkali-earth metal. The t value for the all ceramics synthesized is within the range typical for the perovskite type crystal structure. The variance σ^2 is maximum for the samples having the Sr content $x = 0.45$ and $x = 0.55$.

For all the samples studied, the $\rho(T)$ curves correspond qualitatively to the semiconductor type $d\rho/dT<0$ within the whole T range. The experimental semiconductor conduction character with the $\rho(T)$ dependence similar to the exponential one can be described within the frames of several physical models. The standard thermal activation relationship for semiconducting systems (Arrhenius law) has the form

$$\rho(T) = \rho_\infty \exp\left(E_a/k_B T\right), \qquad (3)$$

where ρ_∞ is a constant corresponding to the conductivity at $T\to\infty$; k_B, the Boltzmann constant. The E_a quantity has the sense of band gap width in the case of band conduction in an intrinsic semiconductor or the sense of activation energy at hopping conductivity over the nearest sites (NSH) in a doped semiconductor [13]. In the latter case, the E_a value is considerably lower [14].

In the frame of variable range hopping conductivity (VRH), the temperature dependence of resistivity has the form

$$\rho(T) = \rho_\infty \exp\left(T_0/T\right)^{1/n}, \qquad (4)$$

where T_0 is the characteristic temperature (the charge carrier localization energy expressed in terms of temperature). The power indices $1/n = 1/4$ and $1/n = 1/3$ correspond to three-dimensional and bidimensinal Mott conductivity, respectively [13]. The relation (2) with the power index $1/n = 1/2$ is considered in the Efros-Shklovsky model [14].

Within the adiabatic approximation of the small polaron hopping model [15], the conduction activation energy is a sum $E_a = E_g/2 + W_H$, where E_g is the charge carrier excitation energy; W_H, the energy necessary for hops. The temperature dependence of resistivity in this case can be expressed as

$$\rho(T) = \rho_0 T \exp\left(E_a/k_B T\right), \qquad (5)$$

where $\rho_0 = k_B/ne^2\omega l^2$, e being the elementary charge; n, the polaron concentration; ω, the optical phonon frequency; l, the polaron hop length.

To identify the conduction type, the experimental results are to be processed in $\ln\rho$ coordinates as a function of $1/T^{1/n}$ ($n = 1, 2, 3, 4$) and $\ln(\rho/T) = f(1/T)$. The rectification of experimental dependences in corresponding coordinates will mean the validity of the model for the sample conductance description.

Our consideration has shown that the conduction nature in the systems studied is different for samples with different strontium content (Figs. 1, 2). As to holmium-containing ceramics (except for $Ho_{0.05}Sr_{0.95}CoO_{3-\delta}$ sample), none of the mechanisms considered is suitable to describe the experimental $\rho(T)$ dependences within the whole temperature range studied. The linear sections appear in the low-temperature part of $\ln\rho(1/T^{1/n})$ curves. The linearity is distorted starting
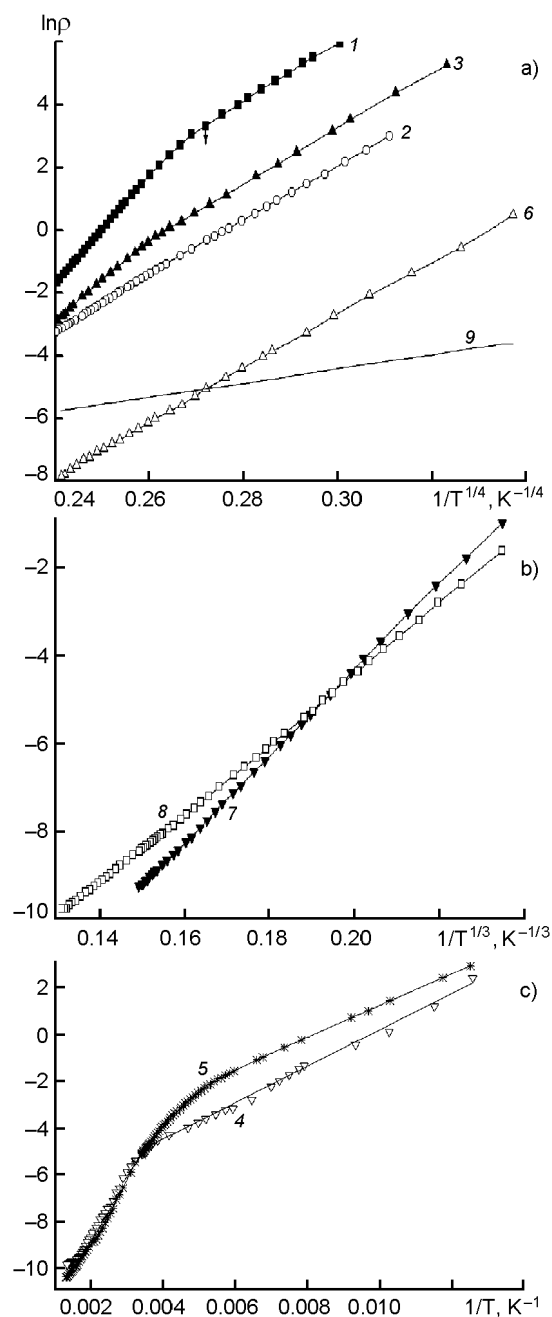
Fig. 1. Processing of experimental $\rho(T)$ dependences for $Ho_{1-x}Sr_xCoO_{3-\delta}$ system samples in the coordinates corresponding to hopping conduction: (a) VRH conductivity, Mott mode, 3D case; (b) RH conductivity, Mott mode, 2D case; (c) NSH conductivity. The x values: 0.15 (*1*), 0.25 (*2*), 0.35 (*3*), 0.45 (*4*), 0.55 (*5*), 0.65 (*6*), 0.75 (*7*), 0.85 (*8*), 0.95 (*9*).

Fig. 2. Processing of experimental $\rho(T)$ dependences for $Er_{1-x}Sr_xCoO_{3-\delta}$ system samples in the coordinates corresponding to VRH conductivity: (a) 3D Mott conductivity; (b) the Efros-Shklovsky mode. Curves are numbered as in Fig. 1.

from the temperature T^* shown by vertical arrows in Fig. 1.

For most samples of $Ho_{1-x}Sr_xCoO_{3-\delta}$ system, the conductivity at $T<T^*$ occurs according to variable range hopping me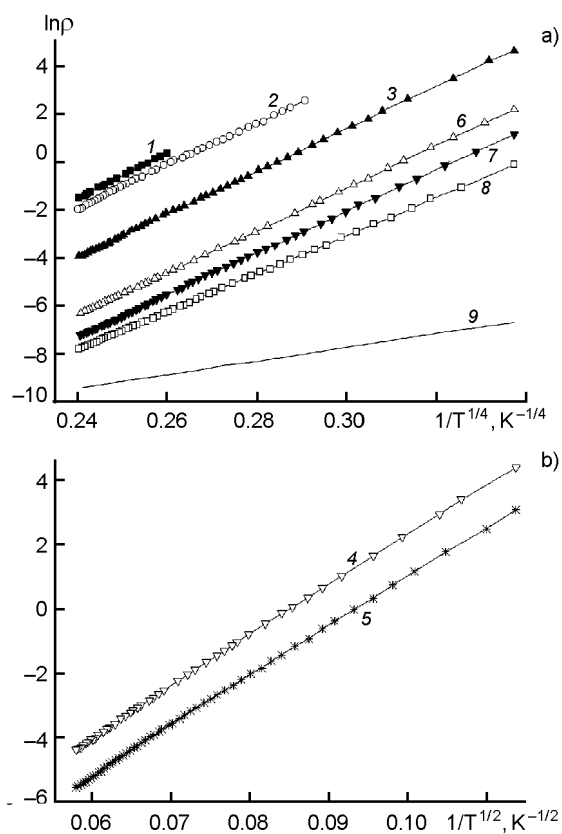chanism of the Mott type. In ceramics with $x =$ 0.15, 0.25, 0.35, 0.65, and 0.95, the Mott law for 3D case is met (Fig. 1a); for $x = 0.75$ and $x =$ 0.85, the 2D Mott conductivity is observed (Fig. 2b; for the $x = 0.85$ sample, the experimental data are processed up to $T =$ 440 K). The samples with strontium doping indices 0.45 and 0.55 form an exception where the conduction is realized by hopping over the nearest sites (Fig. 1c; for those ceramics, the experimental data are obtained and processed up to $T = 770$ K).

The $Er_{1-x}Sr_xCoO_{3-\delta}$ system shows a similar behavior. In ceramics with $x = 0.15$, 0.25, 0.35, 0.65, 0.75, 0.85 and 0.95, the Mott law for 3D case is met (Fig. 2a); while for two samples with the "intermediate" strontium concentration ($x = 0.45$, $x = 0.55$), the Efros-Shklovsky approximation is valid (Fig. 2b).

That result can be explained taking into account that the σ^2 parameter describing the distribution disorder of the A site cat-
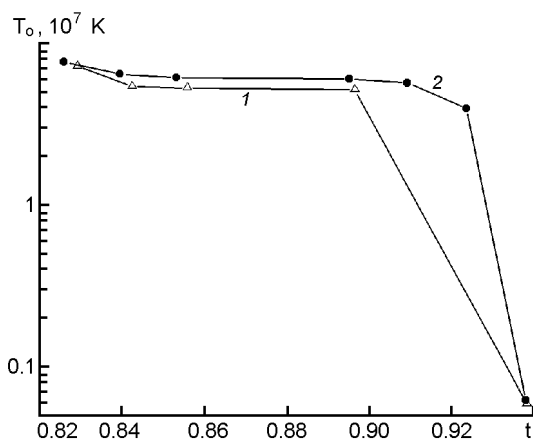
Fig. 3. Characteristic temperature variation as a function of tolerance factor for samples with 3D Mott conductivity: $Ho_{1-x}Sr_xCoO_{3-\delta}$ system (1), $Er_{1-x}Sr_xCoO_{3-\delta}$ system (2).

Table 1. Characteristic temperature T_0 depending on tolerance factor for samples with 2D Mott conductivity

Composition	t	T_0, 10^5 K
$Ho_{0.25}Sr_{0.75}CoO_{3-\delta}$	0.910	9.62
$Ho_{0.15}Sr_{0.85}CoO_{3-\delta}$	0.924	5.37

Table 2. Characteristic temperature T_0 depending on tolerance factor for samples with Efros-Shklovsky conductivity

Composition	t	T_0, 10^4 K
$Er_{0.55}Sr_{0.45}CoO_{3-\delta}$	0.867	2.36
$Er_{0.45}Sr_{0.55}CoO_{3-\delta}$	0.881	2.30

ions attains its maximum at strontium concentration $x = 0.45$ and $x = 0.55$. The maximum σ^2 means the maximum local lattice distortions and periodicity deteriorations of the medium electric potential where the charge carriers move. In the $Ho_{1-x}Sr_xCoO_{3-\delta}$ system, this causes an increased localization, that results in the electron hopping over the nearest sites only. Calculations using the data of Fig. 1c gives the values of E_a included in (3) of 69 meV for $Ho_{0.55}Sr_{0.45}CoO_{3-\delta}$ and 60 meV for $Ho_{0.45}Sr_{0.55}CoO_{3-\delta}$. In the erbium-strontium system, the increased electron structure disorder at $x = 0.45$ and $x = 0.55$ results in a stronger electron-electron interaction and appearance of a Coulomb gap in the localized state density spectrum near the Fermi level. The qualitative difference between conductivity of holmium and erbium samples is like to be connected with the fact that at the same doping level, the $<r_A>$ value in the $Er_{1-x}Sr_xCoO_{3-\delta}$ system is somewhat smaller than in $Ho_{1-x}Sr_xCoO_{3-\delta}$ one, while σ^2 being somewhat larger.

Proceeding from the experimental $\rho(T)$ data processing using Eq.(4) (Figs. 1a, 1b, 2), the characteristic temperature T_0 for the variable hopping conductivity was calculated:

$$T_0 = d(\ln\rho) / d(T^{1/n}). \qquad (6)$$

The T_0 value decreases as the tolerance factor increases for Sr-doped samples with the 3D Mott conduction (Fig. 3). The quantitative differences in the T_0 values for holmium and erbium ceramics with similar tolerance factors are insignificant. The charac-

teristic temperatures for the samples with 2D Mott conductivity and those with Efros-Shklovsky one are presented in Tables 1 and 2, respectively. The trend to T_0 decrease at increasing tolerance factor is manifested in those conductivity modes, too. The obtained T_0 values are typical of similar systems [16, 17].

The mean hopping length R_h and hopping energy E_h were calculated using relationships taken from [18] that are the corollaries from the Mott formulas for 3D conductivity:

$$R_h = (3/8)a(T_0/T)^{1/4}, \qquad (7)$$

$$E_h = (1/4)k_BT^{3/4}T_0^{1/4}, \qquad (8)$$

where a is the decay length of the localized state wave function near the Fermi level (the localization length); in cobaltites, $a = 5 \overset{\circ}{A}$ [17]. As the tolerance factor increases, the mean hop length (being several interatomic distances in the case of VRH conduction) diminishes. Such a regularity is typical of both erbium and holmium samples doped with strontium where the Mott law for 3D conductivity is met (Fig. 4). The E_h varies in a similar manner (Fig. 5). The mean hopping energy value coincides in the order of magnitude with that obtained in [17] for $Y_{1-x}Ca_xCoO_{3-\delta}$ perovskite-like compounds.

The revealed regularities of the tolerance factor influence on the hopping conductivity parameters can be explained as follows. As the $<r_A>$ value grows, the chemical pressure in the system decreases. This causes an elongation of Co–O bonds and reduced the p-d hybridization of cobalt and oxygen elecrton clouds. As a result, the crystal
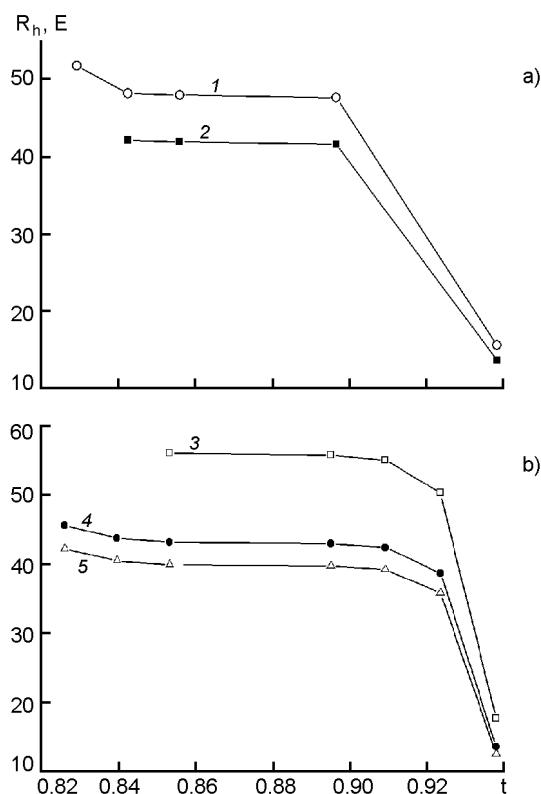
Fig. 4. Mean hopping length variation as a function of tolerance factor for $Ho_{1-x}Sr_xCoO_{3-\delta}$ (a) and $Er_{1-x}Sr_xCoO_{3-\delta}$ (b) ceramics in the temperature range where the Mott law for 3D case is met. Temperature (K): 125 (*1*), 214 (*2*), 77 (*3*), 220 (*4*), 300 (*5*).

Fig. 5. Mean hopping length variation as a function of tolerance factor for $Ho_{1-x}Sr_xCoO_{3-\delta}$ (a) and $Er_{1-x}Sr_xCoO_{3-\delta}$ (b) ceramics at temperatures corresponding to the 3D Mott conductivity. Curves are numbered as in Fig. 4.

field effect becomes reduced, and the energy gap Δ between the t_{2g} and e_g states becomes narrowed. As a consequence, the band of e_g electrons becomes broadened and the localization reduces, thus causing the lowering of characteristic temperatures (both Mott and Efros-Shklovsky ones), the mean hopping length and energy and increase of the localized state density within a narrow band near the Fermi level in the case of Mott conductivity. The differences in the NSH conductivity activation energy (E_a) values for $Ho_{0.55}Sr_{0.45}CoO_{3-\delta}$ and $Ho_{0.45}Sr_{0.55}CoO_{3-\delta}$ samples can be explaned similarly.

The absence of qualitative differences in the structure parameter t influence on T_0 and its derivatives characterizing the VRH conductivity for the erbium and holmium systems is explained by the closeness of Ho^{3+} and Er^{3+} ionic radii. It is to note that at the same doping indices x, the characteristic temperature for the Mott conductivity (Fig. 3) is somewhat higher for erbium samples. This is connected with the somewhat shorter Er^{3+} radius and the resulting
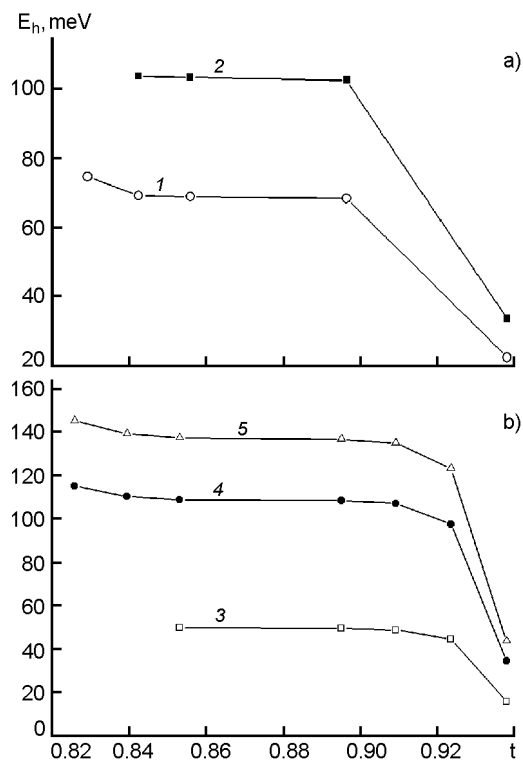
higher value of σ^2 that influences the localization.

For the $Ho_{1-x}Sr_xCoO_{3-\delta}$ system, the deviation of curves *1-6* in Fig. 1 from linearity towards lower ρ values can be interpreted as the appearance of a second conduction channel in the samples. That channel arises at $T = T^*$ in the semiconductor matrix having the VRH conductivity ($x = 0.15$, 0.25, 0.35, 0.65) or NSH one ($x = 0.45$, $x = 0.55$). That is why a model where the samples were presented as two parallel resistors with conductivities σ_1 and σ_2 was used to describe the conductance within the whole temperature range studied. The model of two parallel resistors where one of those has a metal type conductivity while the other is a semiconductor has been considered in [19]. The 2nd conduction channel in $Ho_{1-x}Sr_xCoO_{3-\delta}$ is due to thermal excitation of cobalt ions to the high-spin state resulting in formation of a spin conduction channel.

The sample conductivity in the model under consideration is the total conductivity of two parallel channels,
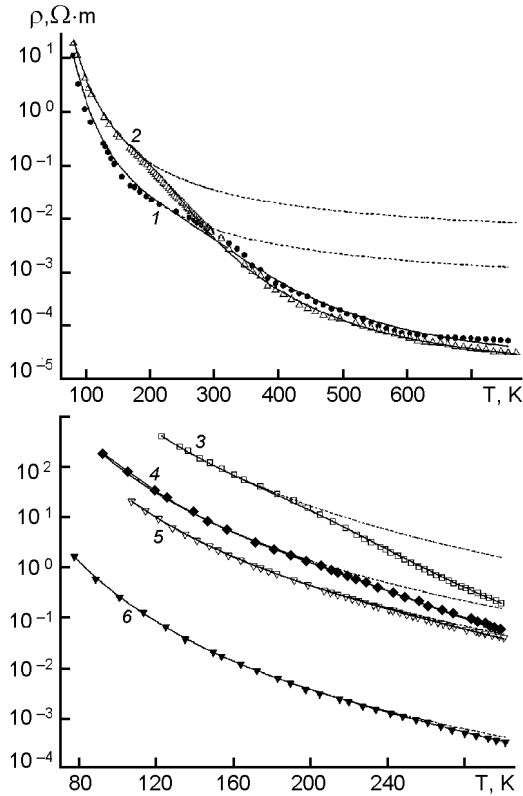
Fig. 6. Fitting of experimental $\rho(T)$ dependences for $Ho_{1-x}Sr_xCoO_{3-\delta}$ system samples corresponding to the dual-channel conductivity model. The x values: 0.45 (*1*), 0.55 (*2*), 0.15 (*3*), 0.25 (*4*), 0.35 (*5*), 0.65 (*6*).

$$\sigma = \sigma_1 + \sigma_2. \qquad (9)$$

The first item corresponds to the semiconductor matrix conductivity occurring according to hopping mechanism. $\sigma_1 = \rho^{-1}$ where ρ is described by (3) for samples with $x = 0.45$, $x = 0.55$ or by (4) for $x = 0.15$, 0.25, 0.35, 0.65. The second item describes the spin conduction channel:

$$\sigma_2 = e\mu n = \sigma_{2\infty}n, \qquad (10)$$

where μ is the e_g electron mobility; $\sigma_{2\infty}$, the conductivity at $T \to \infty$; n, concentration of e_g electrons thermally excited from IS to HS state.The quantity n coincides with function describing the concentration of cobalt ions converted into the high-spins state [20]:

$$n = \nu/[\nu + \exp(\Delta/k_BT)], \qquad (11)$$

where ν is the multiplicity of the Co^{3+} ion excited state; Δ, the spin gap.

It is to note that the temperature T^* of the spin condiction channel appearance for

Table 3. Fitting parameters ρ_∞ and $\sigma_{2\infty}$ in the dual-channel conductivity model for samples of Ho–Sr–Co–O system

Composition	ρ_∞, $\Omega \cdot m$	$\sigma_{2\infty}$, $(\Omega \cdot m)^{-1}$
$Ho_{0.85}Sr_{0.15}CoO_{3-\delta}$	$3.6 \cdot 10^{-10}$	$1.4 \cdot 10^4$
$Ho_{0.75}Sr_{0.25}CoO_{3-\delta}$	$5.2 \cdot 10^{-11}$	$9.5 \cdot 10^4$
$Ho_{0.65}Sr_{0.35}CoO_{3-\delta}$	$1.8 \cdot 10^{-10}$	$1.12 \cdot 10^4$
$Ho_{0.55}Sr_{0.45}CoO_{3-\delta}$	$4.5 \cdot 10^{-4}$	$5.7 \cdot 10^4$
$Ho_{0.45}Sr_{0.55}CoO_{3-\delta}$	$3.5 \cdot 10^{-3}$	$7 \cdot 10^4$
$Ho_{0.35}Sr_{0.65}CoO_{3-\delta}$	$6 \cdot 10^{-13}$	$3.4 \cdot 10^4$

$Ho_{0.45}Sr_{0.55}CoO_{3-\delta}$ and $Ho_{0.35}Sr_{0.65}CoO_{3-\delta}$ samples coincides with the starting temperature of the thermal e.m.f. reduction in those samples that is associated with the charge disproportionality of Co ions that is possible in an excited state only [12]. In the model proposed to describe the temperature dependence of the thermal e.m.f., the fitting to experimental results was possible only with the proviso that the energy difference between the IS and HS states of cobalt ions is small. It is just the multiplicity $\nu = 33$ that mets that condition [21]. Therefore, the fitting using (10) and (11) was carried out at that ν value.

The fitting results are shown in Fig. 6. The solid curves corresponding to the dual-channel conductivity model agree very well with experimental $\rho(T)$ dependences. The dotted lines show the dependences corresponding to the matrix conductivity without the spin channel which are described by the NSH conductivity formulas (Fig. 6,a) and 3D Mott conductivity (Fig. 6b). The temperatures at which the dual-channel curves and single-channel ones start to differ coincide with T^*. The fitting parameters ρ_∞ and $\sigma_{2\infty}$ used to construct the theoretical $\rho(T)$ dependences are presented in Table 3. The order of magnitude coincidence of $\sigma_{2\infty}$ values for the samples with different hopping conductivity types confirms indirectly the same nature of the second conduction channel. The considerable differences between ρ_∞ values for $x = 0.45$, $x = 0.55$ samples as compared to the other ceramica are connected with different conduction characters of the semiconductor matrix. The spin gap width used as the fitting parameter reduces as the tolerance factor increases (Fig. 7). Such a behavior of Δ agrees with the above-considered influence mechanism of the
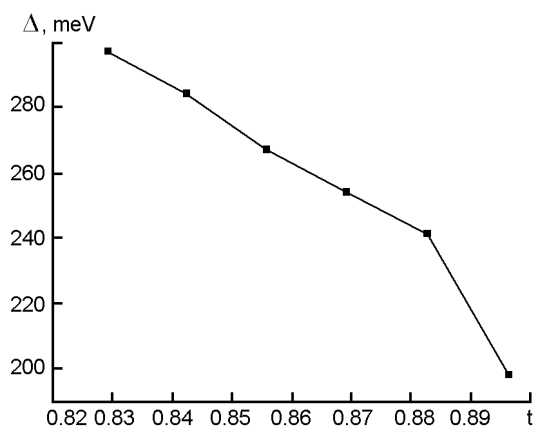
Fig. 7. Spin gap variation as a function of tolerance factor for $Ho_{1-x}Sr_xCoO_{3-\delta}$ samples.

A-site cation mean radius on the hopping conductivity parameters. The Δ values for $Ho_{0.45}Sr_{0.55}CoO_{3-\delta}$ and $Ho_{0.35}Sr_{0.65}CoO_{3-\delta}$ samples coincide with those used in [12] when processing theoretically the temperature dependence of the thermal e.m.f. It is to note that the deviation of the dependences shown in Fig. 1 from the linearity for samples having $x = 0.75$ and $x = 0.85$ is not associated with the opening of a new conduction channel, as it occurs towards the increases resistance.

The presence of excited spin states in the samples does not mean the appearance of a magnetically ordered state. It follows from the magnetic susceptibility measurements that all the samples where a spin contribution to the conductivity is revealed are paramagnetics (as all other samples studied). This may be a consequence of a weak exchange between cobalt ions in the temperature range studied.

The Ca-containing ceramica are characterized by considerably higher ρ values than Sr-containing ones, the substitution indices being the same. That is why the resistance measurements have been carried out therefor at $T<300$ K within a considerably narrower temperature range. For all the samples, the same hopping conductivity is typical of, namely, the 3D Mott conductivity (Fig. 8). This is connected with the fact that the σ^2 parameter in Ca ceramics is significantly lower than in Sr doped ones; moreover, σ^2 depends only slightly on the calcium concentration. The effect of structure parameter t on the hopping conductivity is in agreement with the above mechanism: the characteristic temperature decreases as the tolerance factor rises, and the T_0 value
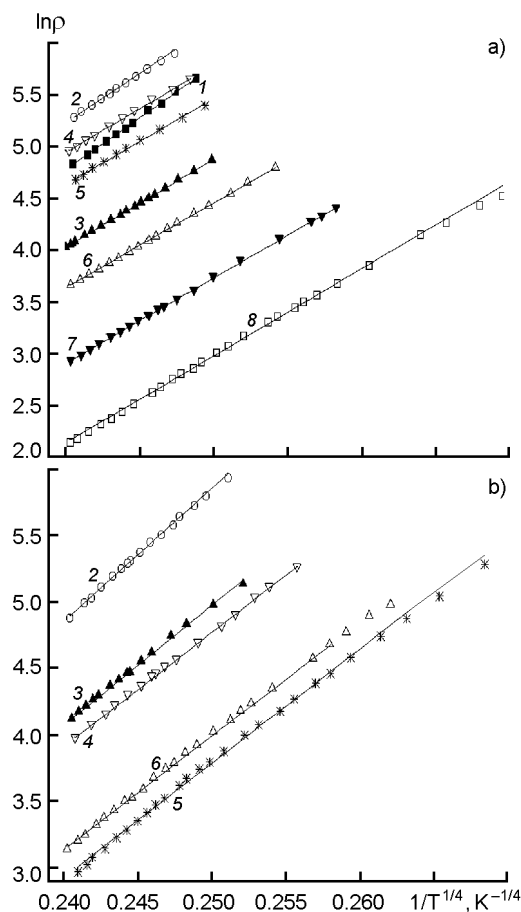

Fig. 8. Processing of experimental $\rho(T)$ dependences in the coordinates corresponding to 3D Mott conductivity mode. (a) $Ho_{1-x}Ca_xCoO_{3-\delta}$ system; (b) $Er_{1-x}Ca_xCoO_{3-\delta}$ system. The x values: 0.15 (*1*), 0.25 (*2*), 0.35 (*3*), 0.45 (*4*), 0.55 (*5*), 0.65 (*6*), 0.75 (*7*), 0.85 (*8*).

is somewhat lower for holmium samples than for erbium ones, the substitution indices being the same (Fig. 9). The characteristic temperature is lower at Ca doping than at Sr one, the rare-earth ion being the same and the tolerance factor values being similar (see Figs. 3 and 9). This difference is due to ionic radii similarity of Ca^{2+} and rare-earth elements as well as the low σ^2 value in Ca-containing samples.

Thus, the consideration carried out has shown that the hopping conductivity type is observed when holmium and erbium cobaltites are doped with alkali-earth elements within a wide range of the dopant concentration. The hop character is defined mainly by disorder that is due to ionic radius mismatch of the A-site cations. At a low σ^2 value (all the Ca-doped samples and those with Sr content $0.15 \leq x \leq 0.35$ and
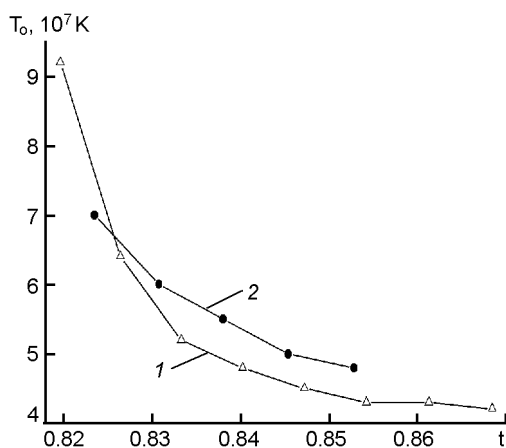
Fig. 9. Variation of the Mott characteristic temperature as a function of tolerance factor for Ca-containing samples. $Ho_{1-x}Ca_xCoO_{3-\delta}$ system (1); $Er_{1-x}Ca_xCoO_{3-\delta}$ system (2).

$0.65 \le x \le 0.95$), the variable range hopping conductivity is realized characterized by a constant local state density within a narrow range near the Fermi level. As the σ^2 value increases up to $\sigma^2 \approx 0.02$ (Sr-doped samples with $x = 0.45$ and $x = 0.55$), the hopping conductivity character is changed. In erbium samples, the disorder of A-site cations causes a correlation effect, a Coulomb interaction between the charges and an energy gap appearance in the localized state spectrum at the Fermi level associated with that interaction. In holmium samples, the localization increase associated with the disorder of A-site cations causes a transition to the hopping conductivity over the nearest sites. The parameters characterizing the hopping conductivity of the same nature (the carrier localization energy, etc.) are influenced mainly by the A-site cation effective radius $<r_A>$. The mechanism of that influence is in connection with the value of chemical pressure causing changes in the energy split of $3d$ levels and spin states of cobalt ions. The main manifestation of that mechanism is the Δ value lowering at increasing tolerance factor that is obtained when processing experimental data within a model taking into account the spin contribution to the conductivity of $Ho_{1-x}Sr_xCoO_{3-\delta}$ system samples. The Mott hopping conductivity parameters that are defined by the localization energy differ always for the samples of different

systems but having similar tolerance factor values. This difference is associated with the fact that the charge carrier states are more localized in samples with a larger ionic radii misfit of A-site cations. Thus, mismatch the σ^2 value influences also the Mott hopping conductivity parameters although to a lesser extent than $<r_A>$.

References

1. A.A.Taskin, A.N.Lavrov, Yoichi Ando, *Phys. Rev. B*, **71**, 134414 (2005).
2. S.G.Ovchinnikov, Yu.S.Orlov, *Zh. Eksp. Teor. Fiz.*, **131**, 485 (2007).
3. V.Golovanov, L.Mihaly, A.R.Moodenbaugh, *Phys. Rev. B*, **53**, 8207 (1996).
4. J.S.Park, S.Y.Park, H.G.Park et al., *J. Korean Phys. Soc.*, **41**, 732 (2002).
5. A.J.Williams, B.M.Sobotka, J.P.Attfield, *J. Solid State Chem.*, **173**, 456 (2003).
6. E.G.Fesenko, Perovskite Family and Ferroelectricity, Atomizdat, Moscow (1972) [in Russian].
7. J.P.Attfield, *Int. J. Inorg. Mat.*, **3**, 1147 (2001).
8. Shengming Zhou, Jun Xu, Guangjun Zhao et al., *J. Phys.:Condens. Mat.*, **16**, 1631 (2004).
9. N.Rama, V.Sankaranarayanan, M.Opel et al., *J. Alloys and Comp.*, **443**, 7 (2007).
10. V.N.Smolyaninova, S.E.Lofland, C.Hill et al., *J. Magn. Magn. Mater.*, **248**, 348 (2002).
11. R.D.Shannon, *Acta Crystallogr. A*, **32**, 751 (1976).
12. V.F.Khirnyi, A.A.Kozlovskii, A.V.Semenov et al., *Functional Materials*, **16**, 150 (2009).
13. N.Mott, E.Davis, Electron Processes in Non-crystalline Materials , Clarendon Press, Oxford (1979)
14. I.B.Shklovsky, A.L.Efros, Electron Properties of Doped Semiconductors, Nauka, Moscow (1982) [in Russian].
15. G. Venkataiah, V. Prasad, P. Venugopal Reddy, *J. Alloys and Comp.*, **429**, 1, (2007).
16. Esa Bose, S. Karmakar, B. K. Chaudhuri, *J. Phys.:Condens. Matter*, **19**, 1 (2007).
17. Y. Liu, X. Y. Qin, *J. Phys. Chem. of Solids*, **67**, 1893 (2006).
18. S. Ravi, Manoranjan Kar, *Phys. B*, **348**, 169 (2004).
19. Masashige Onoda, Asami Sugawara *J. Phys.: Condens. Mat.*, **20**, 1 (2008).
20. Kichizo Asai, Osamu Yokokura, Nobuhiko Nishimori et al., *Phys. Rev. B*, **50**, 3025, (1994).
21. W. Koshibae, K. Tsutsui, S. Maekawa, *Phys. Rev. B*, 62, 6869 (2000).

Вплив толеранц-фактора та безладу A-катіонів на транспортні властивості перовскітів $A'_{1-x}A''_{x}CoO_{3-\delta}$ (A′ = Ho, Er; A″ = Ca, Sr)

А.А.Козловський, В.П.Хірний, О.В.Семенов, В.М.Пузіков, Т.Г.Дейнека, О.В.Гайдук, Ю.М.Цзян

В області температур $T>77$ К досліджено температурні залежності питомого електричного опору керамік $Ho_{1-x}Sr_{x}CoO_{3-\delta}$, $Er_{1-x}Sr_{x}CoO_{3-\delta}$, $Ho_{1-x}Ca_{x}CoO_{3-\delta}$ та $Er_{1-x}Ca_{x}CoO_{3-\delta}$ ($x = 0,15; 0,25; 0,35; 0,45; 0,55; 0,65; 0,75; 0,85; 0,95$), що мають структуру перовскіту ABO_3. Вивчені сполуки характеризуються стрибковою провідністю з температурною залежністю електроопору $\rho(T) = \rho_{\infty}exp(T_{0}/T)^{1/n}$. Залежно від дисперсії розподілу σ^2 радіусів A-катіонів реалізуються різні типи стрибкової провідності. У більшості зразків провідність здійснюється за механізмом стрибкової провідності зі змінною довжиною стрибка у режимі Мотта ($n = 4$). У системі $Ho_{1-x}Sr_{x}CoO_{3-\delta}$ при збільшенні величини σ^2 відбувається перехід до стрибкової провідності поміж найближчими сусідами ($n = 1$); а у системі $Er_{1-x}Sr_{x}CoO_{3-\delta}$ — до режиму Ефроса-Шкловського ($n = 2$). У зразках $Ho_{1-x}Sr_{x}CoO_{3-\delta}$ при підвищенні температури до 190–270 К виявлено появу спінового каналу провідності, пов'язану з переходом іонів кобальту у збуджений стан.